Scientific Annals, School of Geology, Aristotle University of Thessaloniki Proceedings of the XIX CBGA Congress, Thessaloniki, Greece	Special volume 100	297-307	Thessaloniki 2010

FOSSILIZED MICROORGANISMS PRESERVED AS FLUID INCLUSIONS IN EPITHERMAL VEINS, VANI Mn-Ba DEPOSIT, MILOS ISLAND, GREECE

Ivarsson M.[1], Kilias S.P..[2] Broman C.[3] , Naden J.[4] and Detsi K.[2]

[1] *Department of Paleozoology, Swedish Museum of Natural History, Svante Arrheniusväg 9 Box 5000, 105 05 Stockholm, Sweden, magnus.ivarsson@nrm.se*
[2]*Department of Economic Geology and Geochemistry, Faculty of Geology and Geoenvironment, Panepistimiopolis, Zographou, 15784, Athens, Greece, kilias@geol.uoa.gr*
[3] Department of Geology and Geochemistry, Stockholm University, Geoscience Building, Svante Arrhenius väg 8C, 106 91 Stockholm, Sweden
[4] *British Geol Survey, Keyworth NG12 5GG, Notts , U.K.*

Abstract: Fossilized microorganisms preserved as fluid inclusions are found in barite–silica-Mn oxide veins in the marine rift basin-related Quaternary Mn-Ba deposit of Vani, Milos . Basin fill consists of 35-50 m thick sequence of glauconitic sediments sandwiched between volcaniclastic sandy tuffs, and, bedding-parallel barite–Mn oxide(–silica) horizons, pebble horizons, and massive gravel. Exhalative barite-rich deposits characteristic of sea-floor venting, such as white smoker(sulphate) structures in glauconitic sediments, feeder veins, bedding-conformable horizons, and extensive microbial mat- related structures in sandy tuffs, were recognized. The feeder veins host the microfossils and consist chiefly of banded barite and minor colloform quartz, Fe-oxyhydroxides, and hollandite-group minerals and MnO_2 phases, and display epithermal textures characteristic of open-space precipitation. Curvilinear, branched filamentous microfossils with distinct segmentation of septa and a turgid appearance of knob-like outgrowths occur associated with spheroidal spore-like microfossils and small twisted microstructures. Both filamentous and spheroidal microstructures are filled with aqueous (liquid ± vapour) and/or hydrocarbon phases. Oil and solid hydrocarbons in the fluid inclusions may represent decomposed biological material. Chitin was detected by the pigment Wheat Germ Agglutinin conjugated with Fluorescein Isothiocyanate (WGA-FITC) in some of the microfossils, indicating that they are fossilized fungi; a fungal interpretation is further supported by microfossil morphology. Smaller, often twisted filamentous microfossils with a simpler morphology in which chitin was not detected probably represent fossilized prokaryotes and, if so, prokaryotes and eukaryotes co-existed in the geothermal system of Vani. Fluid inclusion microthermometry shows that microfossils were trapped at temperatures of ~100°C in boiling water, probably evolved seawater. Preservation of microfossils occurred at shallow sub-marine conditions of <10 m depth. Our results show that fluid inclusions may contain valuable palaeobiological information and can be used both for establishing biogenicity but also for the reconstruction of the palaeoenvironment of fossilized microorganisms.

Keywords: fossilized fungi, chitin, WGA-FITC, epithermal vein, Milos, Vani

1. Introduction

Submarine, and subaerial volcanic and subvolcanic, hot-springs in both modern and ancient Earth exemplify the links between hydrothermal systems and microbial life (e.g. Harris et al. 2009 and references therein). Microorganisms are a common feature in both extant and extinct hydrothermal environments and recognised as an important agent in hydrothermal related geochemical and biogeochemical processes (e.g. Edwards et al., 2005; Ivarsson et al., 2008 and references therein; Dick et al., 2009). Hydrothermal systems are characterised by high rates of mineralization and may favour preservation of microorganisms which may host organic remains (Ueno et al., 2006). A recent study shows that fossilized microorganisms in combination with coexisting fluid inclusions in hydrothermal precipitates are a successful approach to reconstruct geobiological palaeoenvi-

ronments (Ivarsson et al., 2009). Fluid inclusions contain information about the fluid regime at the time of mineral formation, and microfossil entrapment, and are an excellent indirect tool to put the fossilized microorganisms in a physicochemical and palaeonvironmental context; however, it may be possible, yet very scarcely successful, to obtain biological information directly from inorganically formed fluid inclusions (Ueno et al., 2006).

In this paper we report of fluid inclusion bearing fossilized microorganisms in hydrothermal quartz from epithermal barite–Mn oxide(–quartz, chalcedony) veins of the Vani Mn-Ba, Milos, Greece. This is, to our knowledge, the first time fluid inclusions have been observed in, and described as the main constituent of, fossilized microorganisms. We use oil-bearing fluid inclusions to establish biogenicity of and to characterize the fossilized microorganisms as well as aqueous/vapour fluid inclusions as tools to describe the palaeoenvironment of the fossilized microorganisms. The fossilized microorganisms are interpreted as co-existing eukaryotes (fungi) and prokaryotes (bacteria or archaea).

2. Regional and local geologic setting

Milos is a recently emergent 2 Ma volcano of the Pliocene—modern South Aegean volcanic arc, that documents the transition between the submarine and terrestrial volcanic environments (Fig. 1) (Fytikas et al., 1986; Stewart and McPhie, 2006). Milos island comprises late Pliocene submarine volcanism and late Pleistocene to Holocene subaerial volcanism, which overly Miocene and lower Pliocene carbonate sedimentary successions. The volcanic rocks are calc-alkaline and range from basalt to rhyolite in composition, but are predominantly andesites and dacites. Moreover, Milos has an active high enthalpy geothermal system that vents in the shallow (<100 m) marine and terrestrial environments, and the island as a whole has been hydrothermally active for around 1.5 Ma (Fig. 1). Recent research on Milos island has identified a new metallogenic environment—namely mineralisation and geothermal activity associated with emergent volcanoes. Here—driven by magmatic heat—sea, meteoric and magmatic waters mix to produce geothermal systems that give rise to hybrid volcanic-hosted massive sulphide (VHMS) and continental epithermal mineralization (i.e. Profitis Ilias, Chondro Vouno, Fig. 1)(Kilias et al., 2001; Naden et al., 2005), and a diverse, submarine to terrestrial, suite of young and extremely well preserved mineralized palaeogeothermal systems. The latter are best represented by the Vani Mn-Ba deposit, in NW Milos (Fig. 1). Vani has been considered by previous workers as a stratabound Mn deposit formed by subsea-floor replacement of porous volcaniclastic rocks (Hein et al., 2000; Liakopoulos et al., 2001; Glasby et al., 2005), diagenetic processes (Skarpelis and Koutles, 2004) and submarine hotspring-type processes (Plimer, 2000). The following description is based on Kilias et al (2007), incorporates basic geological data from previous and presents some new data.

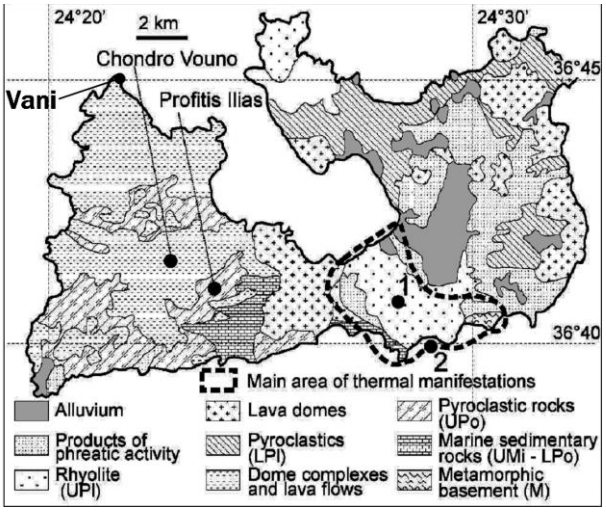

Fig. 1. Main geologic features of Milos Island plus location of Vani, hybrid VHMS-epithermal mineralization (Profitis Ilias and Chondro Vouno) and main surface manifestations of geothermal system—points 1 and 2 show the locations of the deep geothermal reservoir (Zephyria) and main shallow submarine geothermal system (Paleochori Bay), respectively. UPI—upper Pleistocene; LPl—lower Pleistocene; UPo—upper Pliocene; LPo—lower Pliocene; UMi—upper Miocene; M—Mesozoic (adapted from Fytikas et al., 1986 and Naden et al., 2005).

Vani deposit occurs in a 1 km long marine rift basin that was developed in a footwall of andesitic lava dome. The basin fill is 35-60 m-thick and consists of Upper Pliocene–Lower Pleistocene siliciclastic glauconitic sediments sandwiched between lower and upper volcaniclastic sandy tuffs/sandstones, bedding parallel barite–Mn oxide (–quartz, chalcedony) horizons, and lenses, pebble horizons, jaspilitic chert, gravel, capped by cherty mudstone with dessication cracks (Fig. 2). We have been able to recognized extensive microbial–possible cyanobacteria– mat related structures (see Noffke et al., 2001; Noffke, 2009) in the upper-

most sandy tuffs (Figs. 3, 4 and unpublished data); these have a variety of forms including structures on bedding planes (levelled bedding surfaces, microbial mat chips, and mat curls) as well as internal bedding structures (gas domes, thrombolitic and sponge pore fabrics, wavy and discontinuous laminae, and mat slump structures) indicative of nearshore intertidal to shallow-water conditions (Noffke et al., 2001).

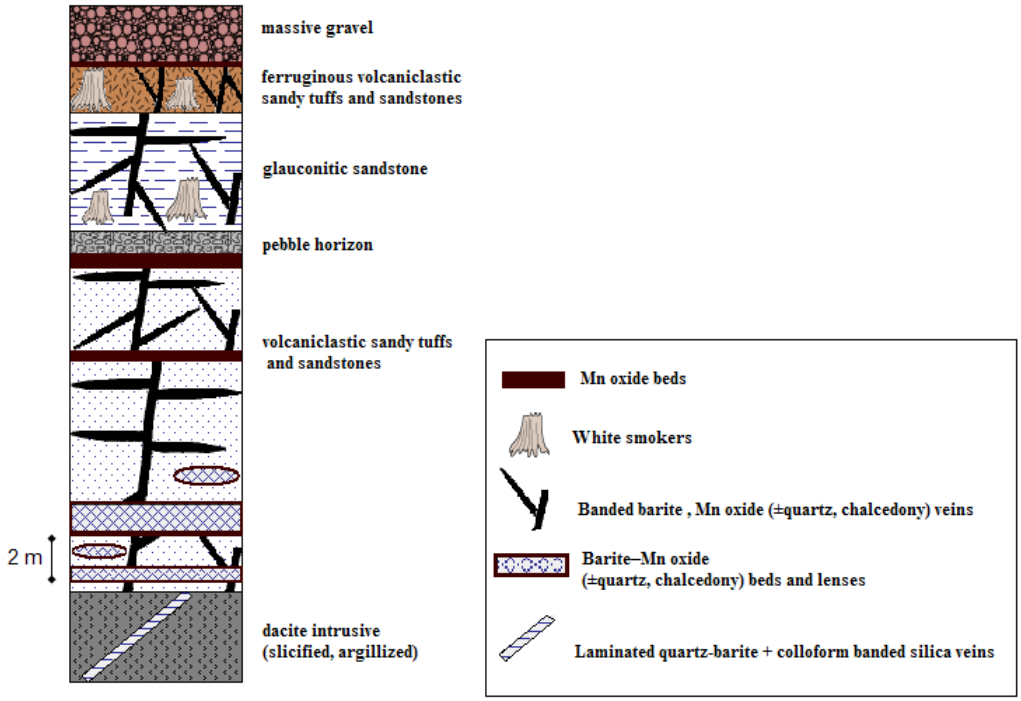

Fig. 2. Schematic stratigraphic section of Vani Mn-Ba deposit (modified after Liakopoulos et al., 2001 and Hein et al., 2000).

There is a important hydrothermal part to the Vani basin development. In addition to the extensive bacterial mats, features characteristic of sea-floor hydrothermal venting, such as white smoker (barite) structures and hydrothermal feeder veins, and hydrothermal mounds, have been recognized in Vani (Figs. 3, 4; Kilias et al., 2007, and unpubl. data). The feeder veins crosscut the sedimentary rocks and consist chiefly of banded open-space-grown of barite and minor colloform quartz, goethite, Fe-oxyhydroxides, and X-ray amorphous hollandite group-like minerals and MnO2–like phases; with the exception of the abundant barite, the vein displays complex and multiepisodic filling with epithermal textures characteristic of open-space precipitation (Hedenquist et al., 2000) (Fig. 3). Discordant colloform-banded epithermal-style stringer veins with the same mineralogy and exhibiting epithermal textures occur for several tens of meters stratigraphically below the sediments within silicified and argillised dacite hangingwall, and hyaloclastite. White smokers have two main modes of occurrence: (1) in massive glauconitic sediments they occur mostly in the form of subparallel vertical pipe-like "white"structures of variable length up to 30-40 cm, and diameter from 2 to 10 cm; individual tubes may have a barite±silica rim and a core filled with hummocky Mn oxide minerals and barite (Fig. 4A), (2) within the upper bedded sandy tuff the white smokers appear "black", and occur in the form of mound-shaped chaotic melange that at places may extend to tens of meters; the melange structure is Mn mineralized and consists of collapsed, toppled, eroded, and brecciated, white smoker chimneys and chimney rubble, debris and fragments, mixed with fragments of fossilised worm tubes, and microbial mat debris, all cemented by Mn oxide minerals and barite. Individual white smoker are hollow tubular structures, some up to 10 -15 cm wide, covered completely by Mn oxide minerals, with rims consisting of concentrically zoned thin Mn oxide layers, and hummocky outer surfaces completely cover by bead-like Mn oxide structures (Fig. 4B, C). Some smokers occur as isolated cylindrical structures consisting of barite-silica±Mn oxide minerals with a hollow core lined with barite ± Mn oxides, and buried in microbial mat debris (Fig. 4D).

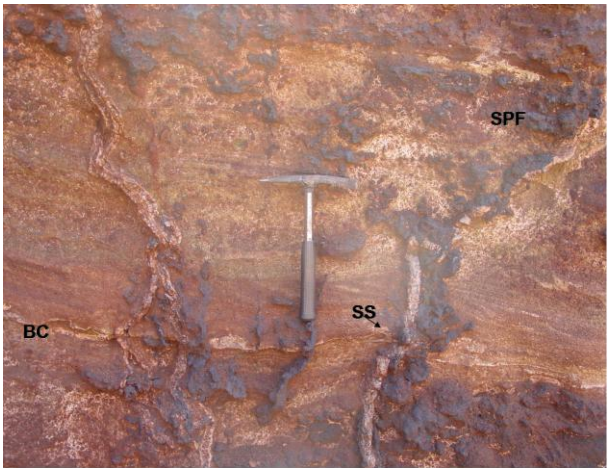

Fig. 3. Host rock of microfossils. Cross section of bifurcating, curvilinear banded barite–Mn oxide(±quartz, chalcedony) epithermal veins crosscutting finely bedded ferruginous sandy tuff, and bedding-conformable horizons with the same mineralogy(BC). Note, possible microbial mat related structures that may suggest syndepositional microbial activity (see Schieber et al. 2007; Noffke 2009): (a) sharply projecting fenestral (sponge pore) fabrics marked by Mn oxides exhibiting cauliflower-like thrombolitic fabrics (SPF)(i.e. biostabilization of the sediments by microbial mats); (b) sinoidal structures(SS) defined by crinkly, wavy and discontinuous barite laminae, denoting biofilm-imprinted rippled bed-surfaces.

The manganese mineralization exhibits a range of deposit styles including white-smoker analogous deposits, subseafloor-replacement and infilling deposits, microbial mat-related deposits, and structurally controlled colloform-banded epithermal-style stringer vein network style (Fig. 3, Kilias et al., 2007). A detailed description of Mn oxide mineralogy may be found in Liakopoulos et al. (2001), and Hein et al. (2000). Manganese minerals were deposited in two stages, and barite formed throughout the duration of Mn oxide mineralization at Vani (Hein et al. 2000; Liakopoulos et al. 2001). The presence of Mn–mineralized microbial mat-related deposits in this shallow marine environmet may suggest the possible role of cyanobacterial photosythesis in Mn^{2+} biooxidation and Mn-oxide biomineralization.

The ubiquitous presence of barite, coupled by the spatial coincidence of feeder-vein and bedding conformable barite-bearing units with white smokers of the same mineralogical composition(Figs. 3, 4), strongly suggest compatibility of the barite-Mn oxide(-silica) units of Vani with low-temperature white smoker (sulphate) deposition (Harris et al., 2009). Furthermore, the gravel unit that caps the Vani sediments contains clasts of dacite, epithermal-style colloform quartz, sandy tuff, manganiferous and ferruginous sandy tuff, and barite. This, coupled with the spatial association of white smokers with microbial mat features preserved within the siliciclastic sediments, suggest that white smoker-type activity, including the feeder veins, have been broadly contemporaneous with sediment accumulation and microbial mat growth in the Vani rift basin(see also Pirajno and Van Kranendonk, 2005). Due to remarkable similarities, Vani may be viewed as a modern analogue for the world's most ancient (3.49 Ga) microbial mats and stromatolites that have developed in association with barite-rich white smoker-type deposits in a shallow-water Early Archean geothermal system preserved in the North Pole Dome, W. Australia (Pirajno and Van Kradendonk, 2005; Harris et al., 2009)

3. Materials and Methods

Extensive fieldwork was conducted between 1996 and 2008 in the broader area around the abandoned open pit mine at Vani, in order to describe and decipher the relationships between sedimentary, hydrothermal and biological phenomena. Vein material for microfossil and fluid inclusion analysis was sampled from outcrops in the open pit. The samples were prepared as doubly polished wafers because these present certain advantages in microfossil studies in terms of better visibility, better light conditions, and an increased 3-dimensional view compared to ordinary thin sections (Ivarsson 2006), due to greater thickness (150–200 μm), and the possibility that the samples could be viewed from both sides.

For Raman spectroscopy analyses, a multichannel Dilor XY spectrometer was used with an incident laser beam of 514.5 nm and an Innova 70 argon laser as a light source.

For the detection of chitin in the microfossils a modified version of the staining method as detailed in Bonfante et al. (1987) was carried out. The pigment Wheat Germ Agglutinin conjugated with Fluorescein Isothiocyanate (WGA-FITC) under fluorescent microscopy was used. This is the first time that such a method is used in geological samples. Chitin is a component in fungal cell walls and not present in the cells of bacteria or archaea and thus WGA-FITC is commonly used to detect fungi or visually separate fungi from bacteria. For the fluorescence we used a Leitz DMRBE epifluorescent microscopy with a Leica DFC 280 camera. Microphotographs are taken in ultra violet light.

Fluid inclusionswere studied in the same wafers. Mirothermometric analyses were carried out using a Linkam TMSG600 heating-freezing stage calibrated using natural carbon-dioxide bearing fluid inclusions of known composition and commercially available chemical standards. Estimated analytical error is ±0.2ºC for low(<50ºC) and ±2 ºC for higher (>75ºC) temperatures.

4. Results and Discussion

4.1 Fossilized Microorganisms

This study has been conducted on barite-quartz interface in barite-Mn oxide(-silica) veins (Fig. 3). The veins consist chiefly of banded open-space-grown of barite and minor quartz, goethite, Fe-oxyhydroxides, and X-ray amorphous hollandite group-like minerals and MnO2–like phases. The barite is enclosed in a fine-grained quartz and has corroded surfaces which indicate that the barite predate the quartz (Fig. 5). Raman spectroscopy shows that the barite, as well as the quartz, is poorly crystalline at the quartz-barite interface. Various types of filamentous and spheroidal microstructures are found preserved in the poorly

Fig. 4. White smokers. A. Massive white smoker-bearing glauconite sandstone, overlying thinly bedded glauconite sandstone . Note white smokers on both sides of the hammer, and pebble horizon with dacite and quartz clasts coated by Mn minerals, at hammers head. The thinly bedded unit contains bedding-conformable barite-Mn oxide(±quartz) horizons; crinkly, wavy and discontinuous laminae may indicate microbial mats. White smokers are vertical, with cylindrical or tubular shape, variable width, and have no structural control; they have a barite and silica rim and a hollow core that may contain Mn minerals. B, C. Collapsed rubble of tubular Mn-oxide coated white smoker chimneys, chimney fragments, and chimney crusts, fossilised worm tubes, and microbial mat destruction structures; the unique microtextures of the Mn oxide deposits and the chimney crusts appear to have been produced by communities of diverse microorganisms inhabiting environments of venting at Vani. D. Isolated hollow barite(silica) white smoker filled with barite. Note cauliflower-like Mn oxides of possible biogenic origin.

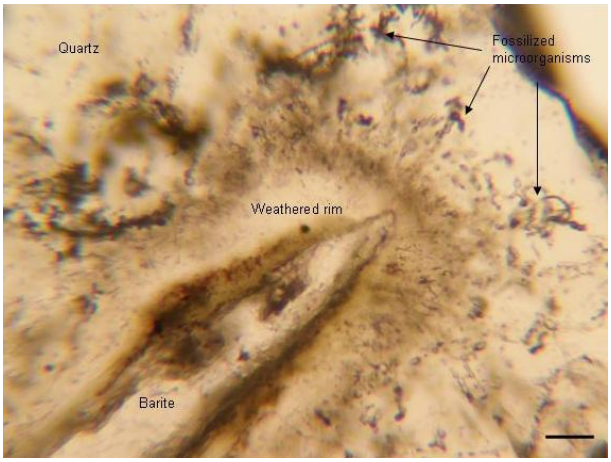

Fig. 5. Microphotograph of the barite-quartz interface. The barite is weathered which indicate that barite predated the quartz. High amount of microstructures at the interface. Scale bar 50 µm.

crystalline fine-grained quartz close to the quartz-barite interface (Fig. 5). The filamentous microstructures vary in size from only ~1 µm in diameter to ~15 µm in diameter (Fig. 6). The length of the small filamentous structures is ~10-20 µm and the length of the larger filamentous structures can range from ~20-200 µm. The morphology of the small filamentous microstructures is simpler with less branching, less segmentation and with a straight or twisted appearance compared to the larger filamentous structures that show more variation morphologically. The large type of the filamentous microstructures is curvi-linear, branched, and with distinct segmentation of septa. Many of the larger filamentous microstructures have a turgid appearance with knob-like outgrowths.

The spheroidal microstructures are between ~5-20 µm in diameter and are either circular or oval in

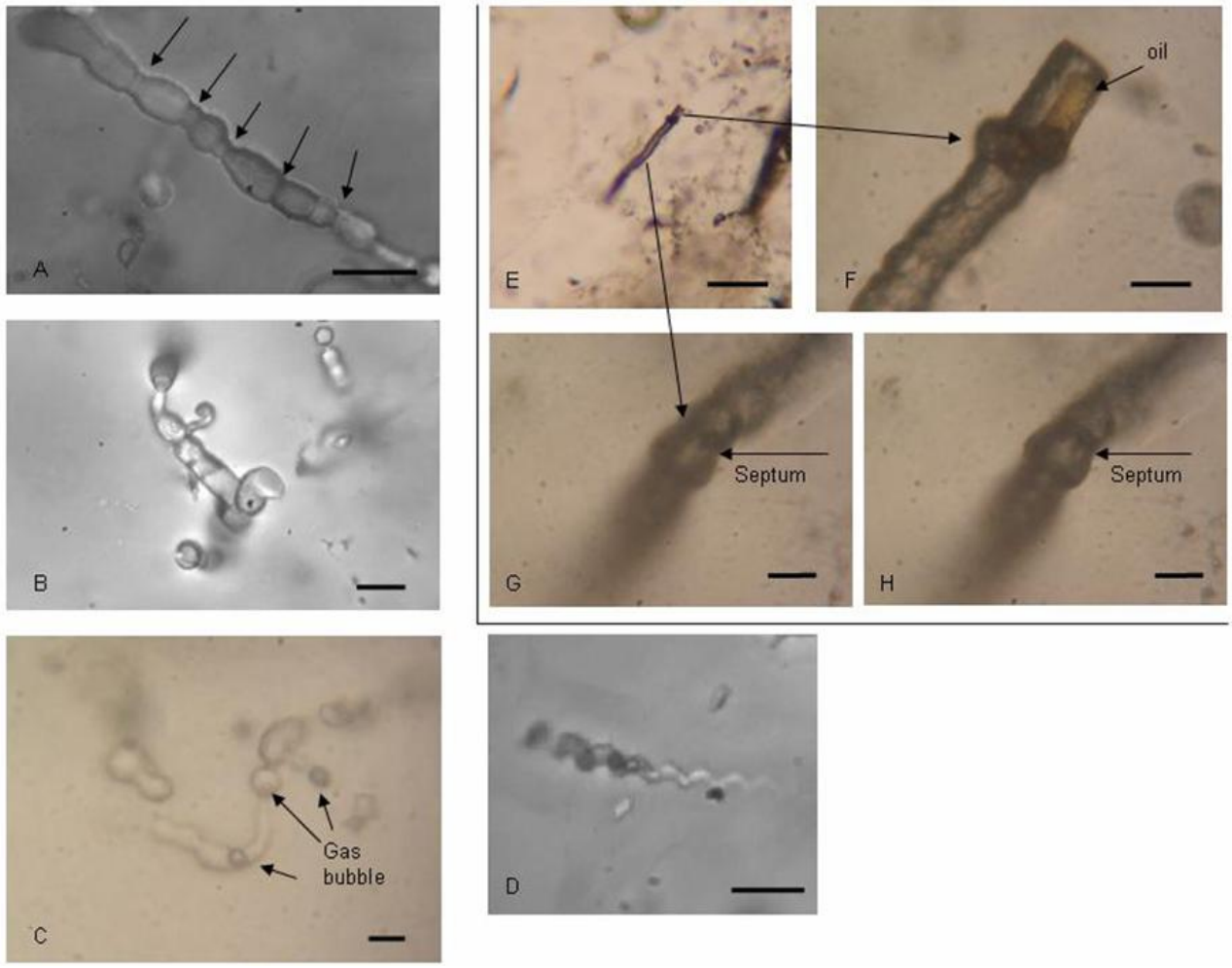

Fig. 6. Microphotographs of filamentous microstructures. A: Large filamentous microstructure with septa. B: Filamentous microstructure with knob-like outgrowths and/or associated spheroidal microstructures. C: Fluid inclusion bearing filamentous and spheroidal microstructures with transitions between the both types. Turgid appearance. D: Small, twisted microstructure. E-H: Large filamentous microstructure divided by septa, with and outgrowth at one end and a one or two phased oil inclusion. Scale bars: A, B, C: 10 µm, D: 5 µm, E: 100 µm, F, G, H: 10 µm.

shape (Fig. 7). Usually, they are bottle-shaped with a tail-like filamentous outgrowth at one end which results in a "spore-like" appearance. The oval microstructures can also be double which results in a "peanut"-like appearance. The spheroidal microstructures are highly associated with the filamentous structures and both types are sometimes combined and form transitions between each other.

Both the filamentous and the spheroidal microstructures are filled with aqueous (liquid ± vapour) and/or hydrocarbon phases. The hydrocarbon phase consists mainly of liquid hydrocarbons, but in a few cases also of solid hydrocarbons that coat the inner walls of the microstructures (Fig. 8). Raman spectra from a brownish solid phase within a filamentous microstructure with Raman bands at 2880, 2850, 1438 and 1295 cm-1 correspond to aliphatic hydrocarbons and may be assigned to evenkite (Jehlicka et al., 2009) (Fig. 9). In some of the larger microstructures chitin was detected with the pigment Wheat Germ Agglutinin conjugated with Fluorescein Isothiocyanate (WGA-FITC) under fluorescent microscopy (Fig. 10). Chitin is a component in fungal cell walls and not present in the cells of bacteria or archaea and thus WGA-FITC is commonly used to detect fungi or visually separate fungi from bacteria. We thus propose that the large microstructures observed represent fossilized fungi. The detection of chitin more or less rules out the possibility that the structures represent fossilized bacteria or archaea. Our interpretation is further supported by the close morphological resemblance with known fungi. The size, septa, branching and turgidity of the filamentous structures correspond more to the morphological appearance of fungi hyphae than filamentous bacteria. The size and morphology of the spheroidal structures are similar to fungal spores or fruiting bodies and their close association with the fossilized hyphae support this interpretation.

The presence of hydrocarbons in the microstructures does not directly support a fungal interpretation but, since the hydrocarbons probably represent thermally decomposed biological material, the presence of hydrocarbons indirectly support the biogenicity.

Microorganisms associated with hydrothermal systems are usually interpreted as prokaryotes belonging to the two kingdoms bacteria or archaea. Fungi are rarely reported from hydrothermal sub-seafloor environments. Marine fungi have been found in deep-sea sediments (Takami, 1999; Nagahama et al., 2003) and in association with hydrothermal vents on the seafloor (López-García et al., 2007) but never below the seafloor. Schumann et al. (2004) reported of fossilized fungi in carbonate filled veins in basalt from the North Pacific Eocene

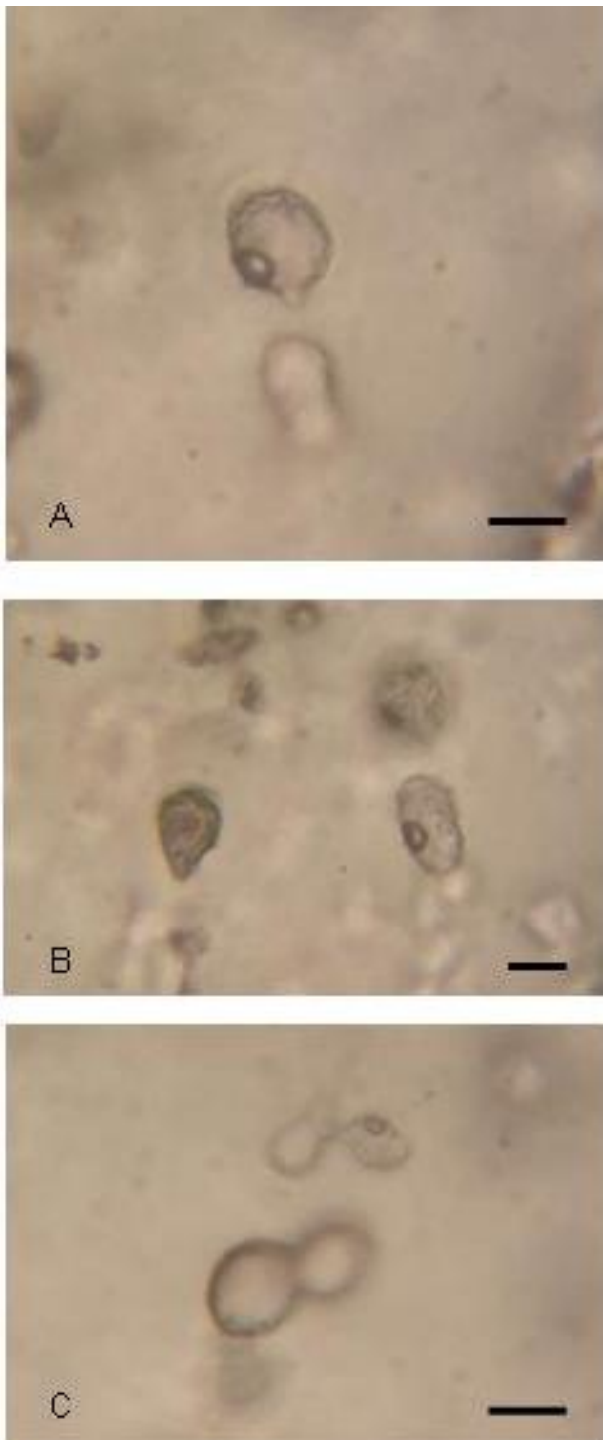

Fig. 7. Microphotographs of spheroidal microstructures. A: Speroidal microstructure with a "spore-like" appearance. B: Oval and "spore-like" microstructures. C: Spheroidal microstructures with a "peanut-like" appearance. Scale bars: A, B, C: 20 µm.

Crust and Reitner et al. (2006) reports of similar filamentous fungi structures in basalts from the Holocene oceanic basement from the Kolbeinsey Ridge (north of Iceland) at a depth of 1500 meters below sea level. These fossilized filamentous structures have been interpreted as fungi based on morphological observations only. The detection of chitin in the samples from Milos, is the first time a specific fungal biomarker has been detected in the fossilized fungi from hydrothermal environments.

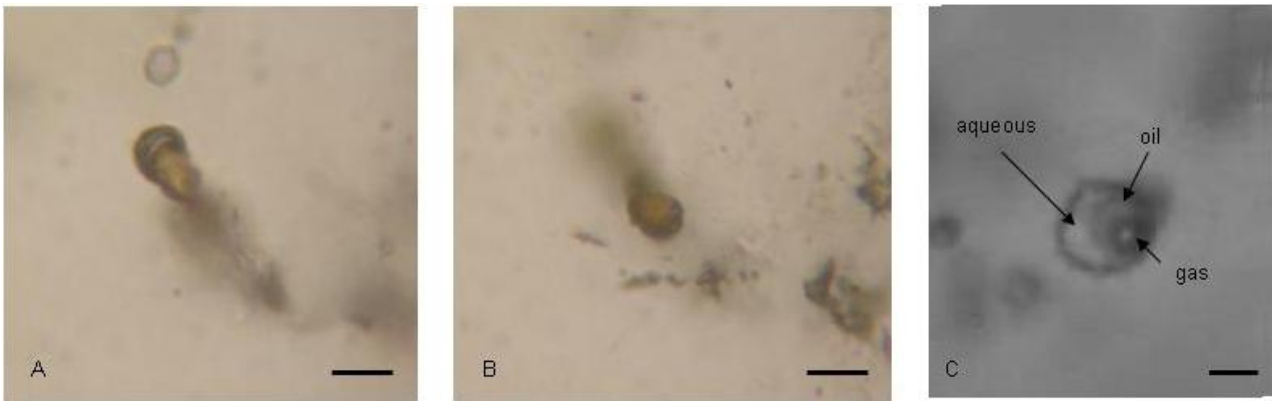

Fig. 8. Microphotograph of oil bearing inclusions. A, B: One or two phased oil inclusions. C: Three phase (gas, oil, aqueous) inclusion. Scale bars: 10 μm.

Fungi are known as an important geobiological agent in terrestrial environments where it lives in symbiosis with bacteria, algae and plants. The occurrence of fungi in sub-seafloor environments indicate that fungi might play an important role in more extreme environments as well, and this will need attention in the future.

The smaller microstructures, in which chitin not was detected, can not be interpreted as fossilized fungi but are most likely fossilized microorganisms as well. We argue this based on (1) the close resemblance morphologically to known microorganisms (Ehrlich 2002), (2) the presence of hydrocarbons, (3) the close association with the fossilized fungi, and (4) that the geological context is compatible with and known to harbour microorganisms (e.g. Harris et al. 2009, and references therein). Lack of chitin is not an evidence for prokaryotes, however, the size and morphology of the smaller microstructures correspond more to prokaryotes than eukaryotes. If this is the case our samples display co-existence between prokaryotes and eukaryotes in a hydrothermal system.

4.2. Fluid Inclusion Microthermometry

Fluid inclusions display the temperature and fluid regime in the system at the time of mineral formation and entrapment of the microorganisms. Small quantities of the hydrothermal mineralising fluid have been captured as fluid inclusions in barite and in the filamentous and the spheroidal microstructures in the fine-grained quartz. In neither of the studied fluid inclusions no signs of post-entrapment modifications like deformation, necking-down or leakage were noted. Microthermometry data on fluid inclusions in barite and the fluid-filled microfossils in quartz are comparable to previous published fluid inclusion data from the shallowest zone of the paleo-geothermal mineralization systems at Milos Island (Kilias et al., 2001; Naden et al., 2005). The present results show that barite was precipitated from a boiling solution at a temperature of around 100°C. Coexisting fluid inclusions have variable liquid/vapour ratios and show a large range of homogenisation temperatures, from 95° to 280°C with homogenisation to both liquid and vapour. This is typical for a heterogeneous system where fluid inclusions have trapped mixtures of various amounts of the residual liquid and the vapour phase. After freezing the inclusions, initial melting was observed within the interval -31° to -45°C, which is below the eutectic temperature of the NaCl-H_2O system and possibly suggests the presence of Ca or Mg salts in addition to NaCl. The final ice melting temperatures were measured between -0.7° (vapour phase dominated) and -12.4°C (residual liquid phase dominated) and correspond to salinities of 1.2 to 16.3 wt. % NaCl eq. (Bodnar, 1993). The aqueous fluid-filled filamentous and spheroidal microstructures in the quartz consist of one phase (liquid) or two phases (liquid and vapour). Homogenization of the two-phase inclusions took place in the range 109° to 144°C, the liquid-only inclusions are believed to have formed at approximately 100°C. The initial melting oc-

curred at similar temperatures as in the barite-hosted inclusions. Final ice melting temperatures were observed between -10.5 and -11.0°C and indicate a salinity of 14.5 to 15.0 wt. % NaCl eq. (Bodnar, 1993).

4.3. The palaeoenvironment and preservation of the microfossils

Our interpretation is that barite formed in boiling geothermal water at 100°C and at a shallow water depth (< 10 m). In previous studies of stable isotopes (D, O, Sr) on fluid inclusions from the epithermal mineralization system at Milos it was concluded that seawater was the main component in the geothermal system (Naden et al., 2005). In the present study, the high salinity of the fluid inclusions in barite is believed to represent the residual liquid phase of boiling seawater and implies that

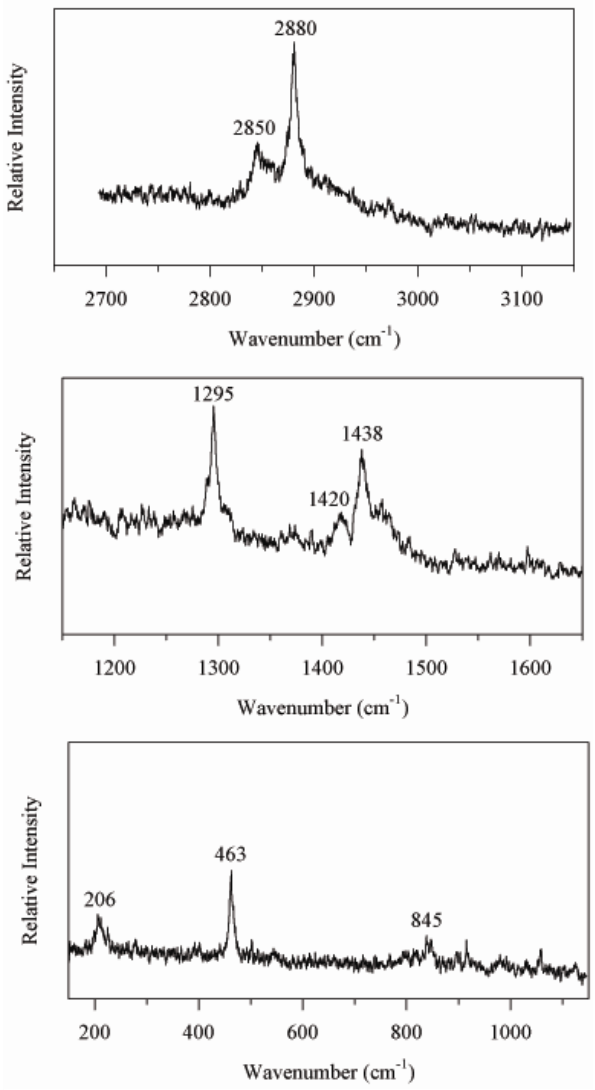

Fig. 9. Raman spectra of a solid hydrocarbon phase coating a microstrcucture.

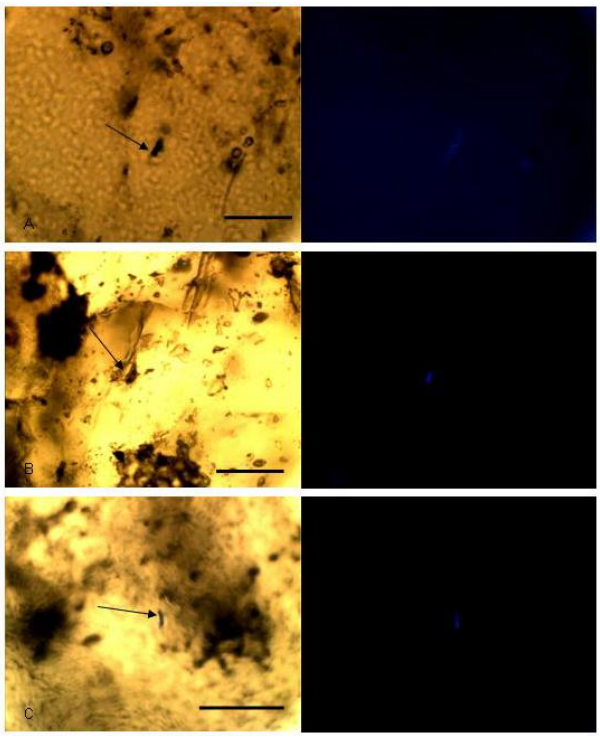

Fig. 10. Microphotographs showing detection of chitin in microstructures by the pigment WGA-FITC. Light microscopy to the left, fluorescence light to the right. Scale bars: 50 μm.

during barite precipitation the salinity of the water gradually evolved from seawater salinity to an elevated concentration (16 wt. % NaCl). The microorganisms were trapped in close association to the barite-quartz interface which suggest that they probably lived in the vicinity of the barite surface. This is supported by the mineralogical similarity of the unconformable feeder and white smoker structures with conformable barite-Mn oxide (–silica) horizons, and geological evidence for their spatial association with microbial mat features preserved within the siliciclastic sediments, which combined may suggest microbial colonization of sites near hydrothermal fluid flow and sea-floor venting. The corroded surface of barite may be the result of microbial sulphate reduction or just altered by the geothermal water. Hydrothermal environments are characterized by sudden pulses of hot fluids that are introduced to the system and it is not clear if the microorganisms existed during active boiling of the hydrothermal system or if they were present at a short period of somewhat cooler conditions. Ivarsson et al. (2009) showed that fluid inclusions associated with fossilized microorganisms do not necessarily represent the temperatures at which the microorganisms lived but merely the temperatures at which the microorganisms were trapped and

preserved. A new discharge of heated silica-rich water flowed into the system, the temperature increased to 100°C and the water started to boil. The silica was deposited as an amorphous accumulation in which the microorganisms were entombed and subsequently decomposed leaving water-filled cavities with preserved shapes of the original microorganisms on the inner walls. Some of the organic matter remained entrapped and still present in the microstructures as the detected liquid and solid hydrocarbons. With time the silica was transformed into the fine-grained poorly crystalline quartz with the microorganisms preserved as fluid inclusions.

5. Conclusions

We have showed how fossilized microorganisms preserved as fluid inclusions can be used in the process of establishing biogenicity of microfossils as well as a tool to describe the palaeoenvironment of the microfossils. Fluid inclusions have previously been suggested as important containers of paleobiological information in combination with the study of fossilized microorganisms (Ivarsson et al., 2009) but fluid-filled microfossils may be even more accurate from a paleobiological point of view and to our knowledge this is the first time it has been reported of. In our opinion these fluid inclusions contain more information than was covered in this paper and our recommendation is to study this type of fluid inclusions more intensely in the future.

Acknowledgements

Financial support from the University of Athens Special Account for Research Grants to S. P. Kilias (KA 70/4/3373, 70/4/6425) and the SEG Hugh Exton McKinstry fund (2006 and 2005) to K. Detsi is gratefully acknowledged. This work was in part funded by the Swedish National Space Board

References

Bodnar R.J., 1993. Revised equation and table for determining the freezing point depression of H_2O-NaCl solutions. Geochimica et Cosmochimica Acta, 57, 683-684.

Bonfante-Fasolo P. , Perotto S., , Testa B. and Faccio A.,1987. Ultrastructural Localization of Cell Surface Sugar Residues in Ericoid Mycorrhizal Fungi by Gold-Labeled Lectins. Protoplasma, 139, 25-35.

Dick G.J., Clement B.G.,. Webb S.M, Fodrie F.J., Bargar J.R., Tebo B.M., 2009, Enzymatic microbial Mn(II) oxidation and Mn biooxide production in the Guaymas Basin deep-sea hydrothermal plume. Geochimica et Cosmochimica Acta, 73, 6517-6530.

Edwards K.J., Bach W. and McCollom, T.M., 2005. Geomicrobiology in oceanography: microbe-mineral interactions at and below the seafloor: Trends in Microbiology, 13, 449-456.

Ehrlich H.L., 2002, Geomicrobiology, Marcel Dekker, New York.

Furnes, H., McLoughlin, N., Muehlenbachs, K., Banerjee, N., Staudigel, H., Dilek, Y., de Wit, M., Van Krankendonk, M., and Schiffman, P., 2008, Oceanic pillow lavas and hyaloclastites as habitats for microbial life through time – a review, in Dilek, Y., Furnes, H., and Muehlenbachs, K., eds., Links between geological processes, microbial activities and evolution of life, Springer, Modern approaches in solid Earth sciences, v. 4, p. 1-68.

Fytikas M., Innocenti F., Kolios N., Manetti P., Mazuolli R., Poli G., Rita F. and Villari, L., 1986. Volcanology and petrology of volcanic products from the island of Milos and neighbouring islets. Journal of Volcanology and Geothermal Research, 28, 297-317.

Glasby G.P., Papavassiliou C.T., Mitsis J., Valsami-Jones E., Liakopoulos A. and Renner R.M., 2005. The Vani manganese deposit, Milos Island, Greece: A fossil stratabound Mn-Ba-Pb-Zn-As-Sb-W-rich hydrothermal deposit. In Fytikas, M. and Vougioukalakis, G.E. (eds), Developments in Volcanology, Elsevier, Amsterdam, v. 7, p. 255-288.

Gold T., 1992, The deep hot biosphere: Proceedings of the National Academy of Sciences, 89, 6045-6049.

Harris A.C., White N.C., McPhie J., Bull S.W., Line M.A., Skrzeczynski R., Mernagh T.P. and Tosdal R.M., 2009. Early Archean hot springs above epithermal veins, North Pole, western Australia: new insights from fluid inclusion microanalysis. Economic Geology, 104, 793-814.

Hedenquist J.W., Arribas A. and Conzalez-Urien, E., 2000. Exploration for epithermal gold deposits. Reviews in Economic Geology, 13, 245-278.

Hein J.R., Stamatakis, M.G. and Dowling, J.S., 2000. Trace metal-rich Quaternary hydrothermal manganese oxide and barite deposit, Milos Island, Greece, Applied Earth Science, section B, 109, 67-76.

Ivarsson, M. (2006) Advantages of doubly polished thin sections for the study of microfossils in volcanic rock. Geochem. Trans. Geochemical Transactions, 7, 1-9.

Ivarsson M., Lausmaa J., Lindblom S., Broman C. and Holm, N.G., 2008. Fossilized microorganisms from the Emperor Seamounts: Implications for the search for a subsurface fossil record on Earth and Mar. Astrobiology, 8, 1139-1157.

Ivarsson M., Broman C., Lindblom S. and Holm, N.G., 2009. Fluid inclusions as a tool to constrain the preservation conditions of sub-seafloor cryptoendolith. Planetary and Space Science, 57, 477-490.

Jehlicka J., Edwards H.G.M. and Vitek, 2009. Assessment of Raman spectroscopy as a tool for the non-destructive identification of organic minerals and biomolecules for Mars studies. Planetary and Space Science, 57, 606-613.

Kilias S., Naden J., Cheliotis I., Shepherd T.J., Constandinidou H., Crossing J. and Simos, J., 2001. Epithermal gold mineralization in the active Aegean Volcanic Arc: the Profitis Ilias deposit, Milos Island, Greece. Mineralium Deposita, 36, .32-44.

Kilias S.P., Detsi K., Godelitsas A., Typas M., Naden J. and Marranitos, Y., 2007. Evidence of Mn-oxide biomineralization, Vani Mn deposit, Milos, Greece. In Andrew et al. (eds), Digging Deeper, Proceedings of the ninth Biennial SGA Meeting, Dublin.

Liakopoulos A., Glasby G.P., Papavassiliou C.T. and Boulegue, J., 2001. Nature and origin of the Vani manganese deposit, Milos, Greece: an overview. Ore Geology Reviews, 18, 181–209.

López-Garcí, P., Vereshchaka A. and Moreira, D., 2007. Eukaryotic diversity associated with carbonates and fluid-seawater interface in Lost-City hydrothermal field: Environmental Microbiology, 9, 546-554.

Naden J., Kilias S.P. and Darbyshire, D.P.F., 2005. Active geothermal systems with entrained seawater as modern analogs for transitional volcanic-hosted massive sulphide and continental magmato-hydrothermal mineralization: The example of Milos Island, Greece. Geology, 33, 541-544.

Nagahama T., Hamamoto M., Nakase T., Takaki, Y. and Horikoshi, K., 2003. Cryptococcus surugaensis sp. nov., a novel yeast species from sediments collected on the deep-sea floor of Suruga Bay. International Journal of Systematic and Evolutionary Microbiology, 53, 2095-2098.

Nora Noffke N., Gerdes G., Klenke T. and Krumbein W.E., 2001. Microbially induced sedimentary structures: A new category within the classification of primary sedimentary structures. Journal of Sedimentary Research, 71, 649-656.

Noffke N., 2009. The criteria for the biogeneicity of microbially induced sedimentary structures (MISS) in Archean and younger, sandy deposits. Earth Science Reviews, 96, 173-180.

Pirajno F., and Van Kranendonk M.J., 2005. Review of hydrothermal processes and systems on Earth and implications for Martian analogues. Australian Journal of Earth Science, 52, 329–351.

Reitner J., Schumann G. and Pedersen K., 2006. Fungi in subterranean environments, in Gadd, G.M., eds., Fungi in biogeochemical cycles, Cambridge University Press, New York, 377-403.

Schumann G., Manz W, Reitner J. and Lustrino, M., 2004.Ancient fungal life in North Pacific Eocene oceanic crust. Geomicrobiology Journal, 21, 241-246.

Skarpelis N. and Koutles, T., 2004. Geology of epithermal mineralization of the NW part of Milos Island: Greece, 5th International Symposium on Eastern Mediterranean Geology, Thessaloniki, Greece.

Stewart A.L. and Mcphie J., 2006. Facies architecture and Late Pliocene – Pleistocene evolution of a felsic volcanic island, Milos, Greece, Bulletin Volcanology, v. 68, p.703-726.

Takami H., 1999. Isolation and characterization of micro-organisms from deep-sea mud, in Horikoshi, K., and Tsujii, K., eds., Extremophiles in deep-sea environments, Springer-Verlag, Tokyo, .3-26.

Ueno Y., Yamada K., Yoshida N., Maruyama S. and Isozaki, Y., 2006. Evidence from fluid inclusions from microbial methanogenesis in the early Archaean era. Nature, 440, 516–519.